J. Fluid Mech. (1980), *vol.* 100, *part* 4, *pp.* 691–703
Printed in Great Britain

Mixing across a density interface produced by grid turbulence

By P. F. LINDEN

Department of Applied Mathematics, University of Cambridge, Silver Street, Cambridge CB3 9EW

(Received 25 May 1979 and in revised form 26 November 1979)

The mixing produced by dropping a horizontal grid through a sharp density interface is examined experimentally. The fraction of the available kinetic energy used to mix the fluid, the flux Richardson number Rf, is measured as a function of the overall Richardson number Ri_0. It is found that Rf increases from zero as Ri_0 does, reaches a maximum, and then decreases with further increase in Ri_0. The final interface thickness is found to be a decreasing function of Ri_0, and the equivalent vertical diffusion coefficient is calculated. Qualitative observations of the flow show that the final stages of the decay of motion in the interface are characterized by pancake-shaped modes with large horizontal and small vertical scales.

1. Introduction

When a fluid in which the mean density gradient is hydrostatically stable is mixed by turbulent motion, work is done by the turbulence against the buoyancy forces. The fraction of the available kinetic energy which is used to do the mixing is known as the flux Richardson number Rf. The remainder of the energy is eventually dissipated by viscosity. There is always some dissipation, and so $Rf < 1$. In an unstratified fluid, as there are no buoyancy forces, $Rf = 0$. As the stratification increases from zero, Rf must also increase from zero. The question of what values Rf takes with further increase in the stratification then arises.

If the strength of the stratification is given by some overall Richardson number Ri_0 (which will be defined precisely later), then the question takes the form of determining the curve of Rf *vs.* Ri_0. Linden (1979) has shown that a number of laboratory experiments can be put into a consistent pattern and it appears that after the initial increase from zero, Rf reaches a maximum of about 0·2 ($\pm$ 0·1) and then decreases again with further increase in Ri_0.

This result has important implications when one considers the evolution of the stratification as a result of the mixing process. As Linden showed, when the turbulence exists uniformly throughout the fluid, Rf is proportional to the vertical density flux and Ri_0 to the vertical density gradient. Thus when Rf increases with Ri_0, regions of high density gradient have large vertical fluxes which tend to reduce the gradients. On the other hand, when Rf decreases as Ri_0 increases, regions of high density gradient support smaller fluxes. Consequently, mass tends to accumulate in these regions leading to even stronger gradients (Phillips 1972; Posmentier 1977). Therefore, the effect of the mixing on the stratification will be quite different depending on which side of the maximum of the Rf *vs.* Ri_0 curve the system lies.

0022-1120/80/4552-2150 $02.00

Although the synthesis of a number of different experiments indicates that Rf does increase to a maximum and then decreases again, no single experiment† showed the whole range of behaviour. Consequently, it is possible that the inferred behaviour was a result of combining different physical configurations rather than intrinsic to an individual one. The aim of this paper is to obtain the complete Rf *vs.* Ri_0 curve for a single experiment.

The main theme behind the design of the present experiment was to try to set up the simplest flow which would allow the direct calculation of Rf. Grid turbulence, about which a great deal is known, was used to mix the fluid. The turbulence was produced by allowing a horizontal grid to fall at terminal velocity through a stationary tank of water. The stratification consisted of two layers of fluid separated by a thin interface. The stability of the system could then be varied quite simply by changing the density difference between the layers. The energy available to mix the fluid is determined by the mass of the grid, and the fraction of it used to mix the fluid was obtained by measuring the stratification before and then again after the passage of the grid through the tank.

As indicated above it is found that Rf increased to a maximum and then decreased again as the stability of the interface Ri_0 increased. A number of other features of the mixing process are also examined. The stratification in the interface is observed to affect the structure of the turbulent motions, the vertical scale of these motions is reduced and pancake-shaped modes, with large horizontal scales, are observed. The final thickness of the interface is found to be a decreasing function of Ri_0, providing a further example of how the stratification inhibits vertical mixing. At low values of Ri_0 these results are expressed in terms of a vertical diffusion coefficient which is in agreement with the form of other estimates for stratified turbulence.

2. The experiments

The experiments were carried out in the following way. Two layers of fluid separated by a sharp interface were placed in a tank. The fluid in the upper layer was fresh water, and the lower layer was a denser, salt solution. Both layers were of equal depth and at room temperature. The vertical density profile was measured once the tank was filled. Then a horizontal grid was allowed to fall freely from rest, under gravity from the surface to the bottom of the tank. When all the ensuing motion had died away the vertical density profile was measured once more. By comparing these two density profiles it was possible to calculate the change in potential energy of the stratification caused by the passage of the grid.

The vertical density profile was measured either by withdrawing samples (1 ml) at predetermined depths and measuring their refractive index, or by using a conductivity probe to measure the salt concentration. The latter method was more accurate when the density difference between the two layers was small but, owing to the nonlinearity of the conductivity probe at high concentrations, the refractive index proved to be more accurate at larger density differences.

The first set of experiments was carried out in a rectangular, perspex tank 25·4 cm

† The exception was the present experiment, some preliminary results of which were given in Linden (1979).

square in cross-section and filled to a depth of 37 cm, (i.e. each layer was 18·5 cm deep). The grid used consisted of a 5×5 rectangular array of square bars in a single plane. Each bar was 1 cm square in cross-section and the distance between the centres of the bars was 5 cm, giving a grid solidity of 0·36. The ends of the bars had a 0·2 cm clearance from the sides of the tank. The grid was positioned by the use of a 0·5 cm diameter vertical, stainless steel rod fixed along the centre-line of the tank. A close fitting brass sleeve was placed in a hole in the centre of the grid, which allowed it to fall freely down the rod without hitting the sides of the tank, and caused it to remain horizontal.

In order to investigate the effects of changing the scale, a set of experiments was carried out in a larger tank. This tank was 58·4 cm square in cross-section and was filled to a depth of 170 cm. A grid of exactly the same geometric shape was used. It consisted of a 5×5 array of square bars 2·3 cm in cross-section, with 11·5 cm between centres. As in the small tank the grid was constrained to remain horizontal and to fall vertically by a 1·2 cm diameter rod placed along the centre-line of the tank.

The grids were constructed from polypropylene, a material which floats in water. They were weighted by placing cylindrical brass weights, which would slide along the rod, on the upper side of the grid. The cross-sections of the weights were smaller than the area of the interaction of the central bars of the grid and so they did not alter the solidity of the grids.

Qualitative observations of the mixing produced by the passage of the grid through the interface were made with a shadowgraph, dye and using neutrally buoyant particles. Some examples of these will be shown in the next section.

Quantitatively, the mixing can, in principle, depend on the following variables: $\Delta\rho$ the density difference between layers, H their depth, g the gravitational acceleration and the molecular properties of the fluid, namely, ν the kinematic viscosity and κ the diffusivity of the solute. It can also depend on the properties of the grid: m its submerged mass, b the width of the bars and M the mesh length. From these quantities we can define the following non-dimensional parameters:

$$\left.\begin{aligned} &\text{Richardson number} && Ri_0 = \frac{g\Delta\rho M}{\rho U^2}; \\ &\text{Reynolds number} && Re = \frac{UM}{\nu}; \\ &\text{Prandtl number} && \sigma = \frac{\nu}{\kappa}; \\ &\text{Grid aspect ratio} && \frac{b}{M}. \end{aligned}\right\} \tag{2.1}$$

In these parameters U is the terminal velocity of the grid in fresh water given by

$$U = \left(\frac{2gm}{\rho C_D A}\right)^{\frac{1}{2}}, \tag{2.2}$$

where C_D is the drag coefficient for the grid and A the cross-sectional area of the tank. In practice, U was measured *in situ* and C_D inferred from (2.2). The values of C_D obtained in this way were 1·60 and 1·63 for the large and small grids, respectively. These values are consistent with drag coefficients for grids of comparable solidity

obtained from measurements in wind tunnels (see Hoerner 1965; Naudascher & Farell 1970). Both grids reached terminal velocity well before reaching the interface and so U is the only relevant velocity scale.

In these experiments we have concentrated primarily on the effects of the strength of the stratification as described by Ri_0. Some attempts to look at the effects of changing Re have been made by comparing results obtained in the large tank ($Re = 1{\cdot}6 \times 10^4$), with those in the smaller tank ($Re = 5{\cdot}1 \times 10^3$).

In all the experiments reported in this paper the interface between the two layers is nominally 'sharp'. The upper layer was carefully floated onto the lower layer by pouring fluid onto a floating sponge. The grid was dropped as soon as practicable after the tank was filled. The elapsed time between the initial addition of upper layer fluid and the passage of the grid was typically 30 min (small tank) and 120 min (large tank). In this time molecular diffusion will have thickened the interface (90 % thickness) to 0·6 cm and 1·2 cm, respectively. This distance is small compared with the mesh size of the grids.

3. Qualitative results

The effects of dropping the grid through the interface are illustrated by referring to a set of shadowgraph observations showing the sequence of events. Figure 1 (plates 1 and 2) shows a typical sequence. In figure 1 (*a*) we see the bright band indicating the presence of the sharp interface which becomes disturbed just before the grid reaches it (figure 1*b*). From the succeeding pictures we see that fluid is both ejected upwards into the upper layer and dragged across the interface into the lower layer in the wakes of the bars of the grid. This fluid then mixes with the fluid surrounding it and moves under its own buoyancy back to the vicinity of the interface. The resulting motion is complicated, internal waves are generated, and the shadowgraph reveals a large amount of small-scale structure. When the motion appears to have ceased (figure 1*e*) there is still some structure in the form of horizontal striations in the stratification. These striations apparently decay by molecular diffusion (figure 1*f*). The final result is that the interface has been smeared out by the mixing.

This sequence can also be seen on the density profiles. Figure 2 shows tracings of a set of profiles taken at $Ri_0 = 0{\cdot}15$ by moving the conductivity probe downwards through a region of the tank spanning the original interface. The probe traverse was only about half the total tank depth, as can be seen by the depth scale. Figure 2 (*a*) shows the initial interface separating the two uniform layers. Figure 2 (*b*) taken about 10 s after the grid has passed through the interface shows evidence of mixing by the presence of small scale density inversions. Figures 2 (*c*) and 2 (*d*) taken at later times show the way in which the density profile smooths out with time.

Streak photographs of aluminium particles suspended in the flow also reveal a number of interesting features. Two examples are shown on figure 3 (plate 3) for a Richardson number $Ri_0 = 3{\cdot}63$. Figure 3 (*a*) is a 2 s exposure after the grid has passed through the interface. The motion is quite different in the region of density gradient near the middle of the tank compared with that in the relatively homogeneous layers on either side. In the layers the motion appears to be typical of the eddying motion produced by grid turbulence in an unstratified fluid. The interface region, however, is characterized by the horizontal bands clearly visible on the photograph. The velocities

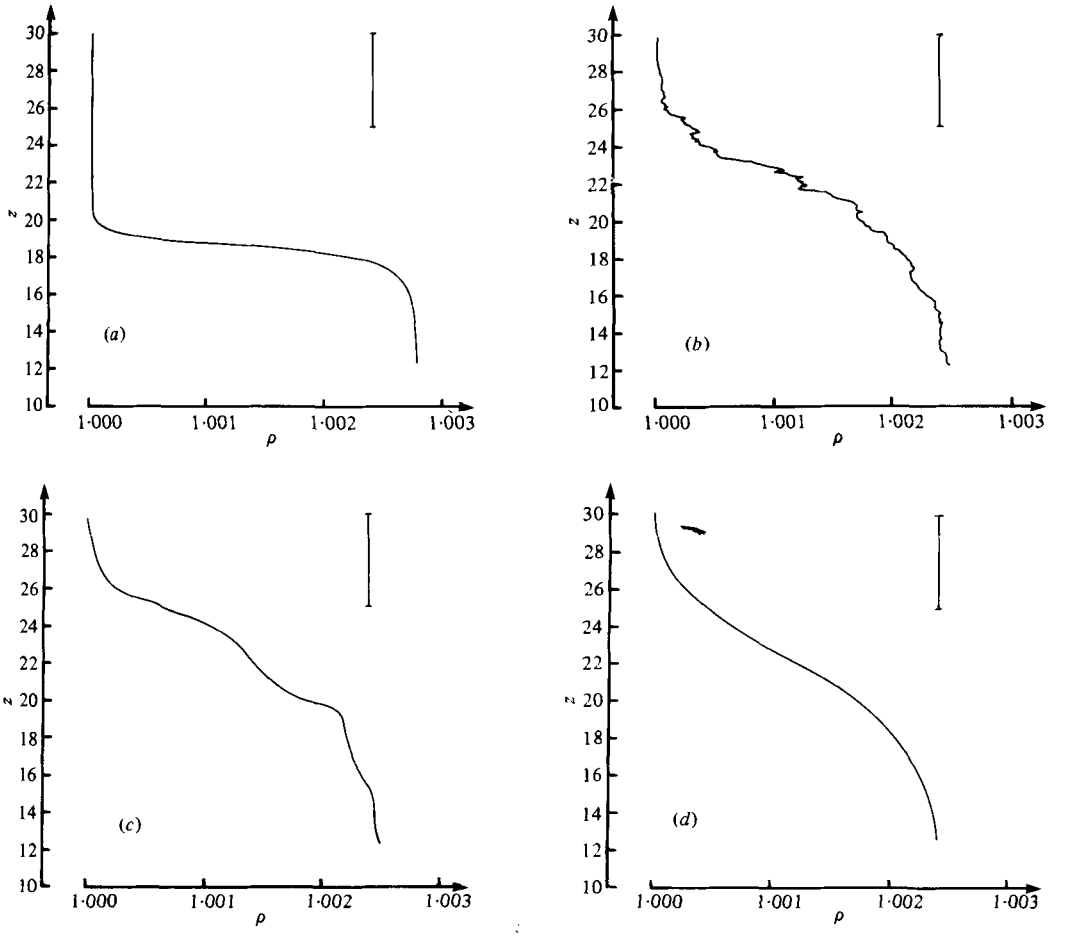

FIGURE 2. Density profiles for $Ri_0 = 0{\cdot}15$ obtained with the conductivity probe taken before (*a*) and then 10 s (*b*), 2 min (*c*) and 5 min (*d*) after the grid is dropped. The vertical scale is in cm measured from the bottom of the tank, whilst the vertical line represents the mesh size of the grid.

in this region are much smaller than in the layers. Figure 3(*b*) is an 8 s exposure of the same experiment taken some 3 minutes after the passage of the grid. The same features are also visible on this photograph, although, as expected, the length scale of the turbulent motions in the layers has increased considerably during the decay. A feature of this photograph is that the thickness of the region marked by the pronounced horizontal bands is thinner than in figure 3(*a*). The vertical extent of this region ($\sim$ 2 cm) is now comparable with the observed thickness of the interface as determined from the density profile (see figure 6). The large-scale horizontal modes in the region of vertical density gradient are the expected form of the motion in the final stages of decay of the turbulence. Pearson (1980) argues that these horizontal modes obtain energy from potential energy which is temporarily stored in the stratification during a mixing event.

These horizontal striations seem to be the same as the horizontal structure seen on the shadowgraph (figure 1*e*). They appear to be more regular in the streak photo-

graphs, but this is due to the method of visualization since the shadowgraph produces an integrated effect across the whole interface, whereas the streak photographs show a thin slice through the tank.

4. Flux Richardson number

The evaluation of the flux Richardson number Rf requires a knowledge of the change in potential energy of the stratification due to the mixing produced by the grid. This is done by evaluating the potential energy per unit area of the water column,

$$V = \int_0^H gz\rho(z)\,dz,$$

where H is the depth of water in the tank, from measured profiles of the density $\rho(z)$ before and after the grid has passed through the interface. The 'after' profile was measured about 20 minutes later when all significant motion had ceased. Over this short time molecular diffusion has a negligible effect on the large scale of the interface region. The integration was carried out numerically, by Simpson's rule, either directly from the density measurements on the runs in which samples were taken, or from digitizing the calibrated conductivity-depth record. In the latter case the profiles were digitized at different depth resolutions to ensure the numerical integration was accurate.

These calculations are subject to large uncertainties as it is necessary to find the relatively small difference between two large numbers. A check on the accuracy was obtained by calculating the total mass of the water column per unit area,

$$\mathscr{M} = \int_0^H \rho(z)\,dz.$$

Only runs were considered in which this was conserved to within 2 parts in 10^{-4}, and which agreed within the same limits, with the value of $\mathscr{M}$ obtained from the depths and densities of the layers added initially. Even so the estimate of the change in potential energy is only guaranteed accurate to within 50 % in the cases when there is little change. Error bars are given in the figures to indicate the uncertainty in calculating the change in V.

The calculation of Rf also requires an estimate of the energy in the turbulence which is available to mix the fluid. The total energy per unit area input into the turbulence by the grid during its fall through distance H is given by mgH/A, where m is the submerged weight of the grid and A is the cross-sectional area of the tank. (The frictional losses along the central rod are negligible.) Clearly, not all of this energy is necessarily available for mixing. Consider the hypothetical case where the interface was positioned at $z = 0$, but the two layers were infinitely deep. Then $H \to \infty$, and the total energy in the turbulent field is infinite. Of course, only the turbulence in the vicinity of the interface can alter the potential energy of the stratification, and it is this (finite) fraction that is of interest.

In order to calculate the fraction of the total energy available to mix the fluid it is helpful to consider the nature of grid turbulence. If the tank is unstratified the passage

of the grid produces, after a short time (about 4 s in the small tank and 8 s in the large tank), approximately isotropic, homogeneous turbulence which decays with time. If fluid across the cross-section was marked immediately after the passage of the grid, then this marked fluid would be dispersed longitudinally during the decay of the turbulence. The final vertical (or longitudinal) extent of this cloud of marked particles is a measure of the maximum fraction of the fluid in the tank which could participate in the mixing of fluid at an interface. Thus this final thickness of the cloud D will be used to calculate the energy per unit area mgD/A available to change the potential energy of the stratification.

It seems impossible to measure D directly with the present arrangement, but it can be inferred from diffusion measurements made in a wind tunnel. Townsend (1954) showed experimentally that the variance S^2 of the lateral spread of temperature behind a heated wire in a wind tunnel can be described by a relationship of the form

$$\frac{S^2}{M} = C(X - X_0), \tag{4.1}$$

where X_0 is the downstream position of the wire and C is a constant with a numerical value of $0{\cdot}06 \pm 0{\cdot}01$. If the turbulence is isotropic, which is a good approximation for grid turbulence, (4.1) can be used to give an estimate of D. It is supposed that (4.1) is valid until the final period of decay sets in, after which further dispersion is assumed to be negligible. The validity of (4.1) holds for $X/M \lesssim 200$ for $Re \sim 600$ (Batchelor & Townsend 1948) and $X/M \lesssim 800$ for $Re = 48000$ (Dickey & Mellor 1980). In the present experiments $Re = 5000$–16000 and, on the basis of interpolation, we take $X/M \lesssim 300$. Hence we get $S/M = 4{\cdot}2$. An appropriate measure of D is twice the standard deviation of the dispersion which gives $D/M = 8{\cdot}4$. We shall use this value throughout the remainder of the paper.

Then the flux Richardson number is defined as

$$Rf = \frac{V_{\text{after}} - V_{\text{before}}}{mgD/A}, \tag{4.2}$$

and we plot the results in terms of the overall Richardson number Ri_0. The results are shown on figure 4. They show that as Ri_0 increases Rf increases to a maximum value $Rf = 0{\cdot}12 \pm 0{\cdot}01$ at $Ri_0 = 1{\cdot}3$. With further increase in Ri_0 the flux Richardson number decreases, showing that in very stable situations the mixing of fluid is strongly inhibited by the stratification.

It is important to emphasize that although the *absolute values* of Rf given by (4.2) depend on the value of D chosen, provided the depth of the tank is greater than D the *shape* of the Rf *vs.* Ri_0 curve is unaltered. Therefore, the implications of the shape of the Rf curve do not depend on the somewhat dubious arguments used to obtain numerical estimates of Rf. Finally, it should be noted that the errors bars on figure 4 reflect uncertainties in the potential energy calculations only. The scale D is assumed to be without error and no account has been taken of the uncertainties involved in (4.1) or the lack of isotropy of grid turbulence.

It is possible to avoid the difficulty of estimating D by presenting the same data in a different way. If we set $Rf = 1$ in (4.2) then we have an equation for D, which, in this case, is the distance the grid must fall in order to supply the energy required for the

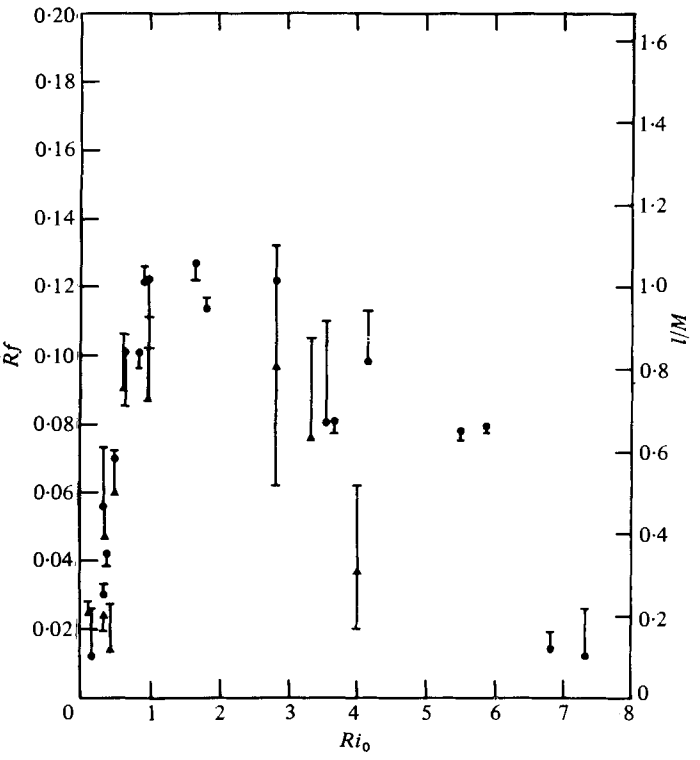

FIGURE 4. The flux Richardson number Rf plotted against the overall Richardson number Ri_0 ●, $Re = 5{\cdot}1 \times 10^3$ (small tank); ▲, $Re = 1{\cdot}6 \times 10^4$ (large tank). The vertical errors bars represent uncertainties in determining Rf due to inaccuracy in the density measurements. Also shown on this figure are the values of the distance l the grid must fall in order to supply the energy required for the observed amount of mixing. The length l has been non-dimensionalized by the mesh length M of the appropriate grid.

observed change in potential energy of the stratification. We denote this distance by l, non-dimensionalize it by the mesh length M, and the values of l/M are also shown on figure 4.

Within the experimental uncertainties the results of the two grids collapse onto a single curve. Therefore, the Reynolds number seems high enough so that there is not a strong dependence on it. This agreement also implies that dissipation on the side walls is negligible and that the tanks are deep enough to ensure that the depth does not seem to limit the energy available to mix the fluid. This is reassuring because although for the large tank $H/M = 14{\cdot}8$, for the small tank $H/M = 7{\cdot}4$ which is uncomfortably close to D/M. We also note that at its maximum value, $l/M = 1{\cdot}0$. Dickey & Mellor (1980) measured the integral scale of grid turbulence during the decay until a time $Ut/M = 1100$, and if we use their results during the estimated period of decay for the present experiments ($Ut/M < 300$), then it appears that the integral scale l is approximately equal to the mesh length ($l/M = 1{\cdot}1$ at $Ut/M = 300$). Thus the maximum value of l is roughly equal to the integral scale of the turbulence. For small values of Ri_0, the density profile also exhibits variations on a length scale comparable with the integral scale, see figure 2(*c*) for which $Ut/M \sim 280$.

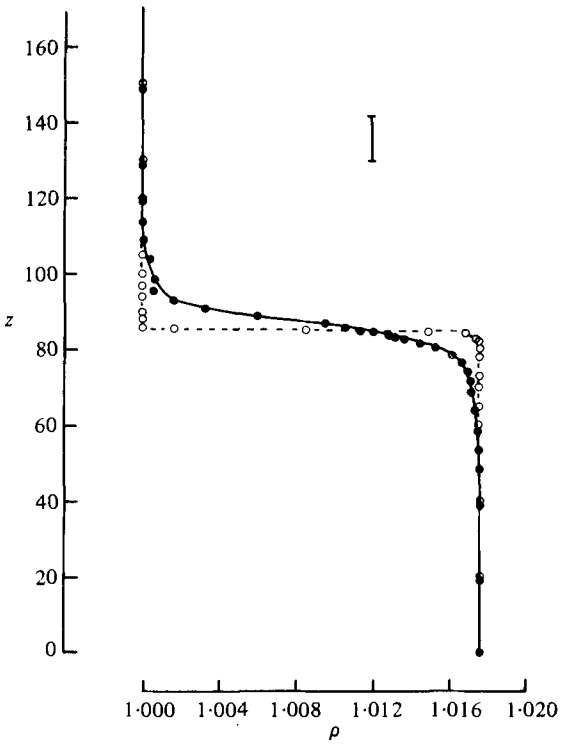

FIGURE 5. Density profiles measured in the large tank before ○ and after ● the passage of the grid for $Ri_0 = 0{\cdot}98$. The depth scale is in cm measured from the bottom of the tank and the vertical bar represents the mesh size of the grid.

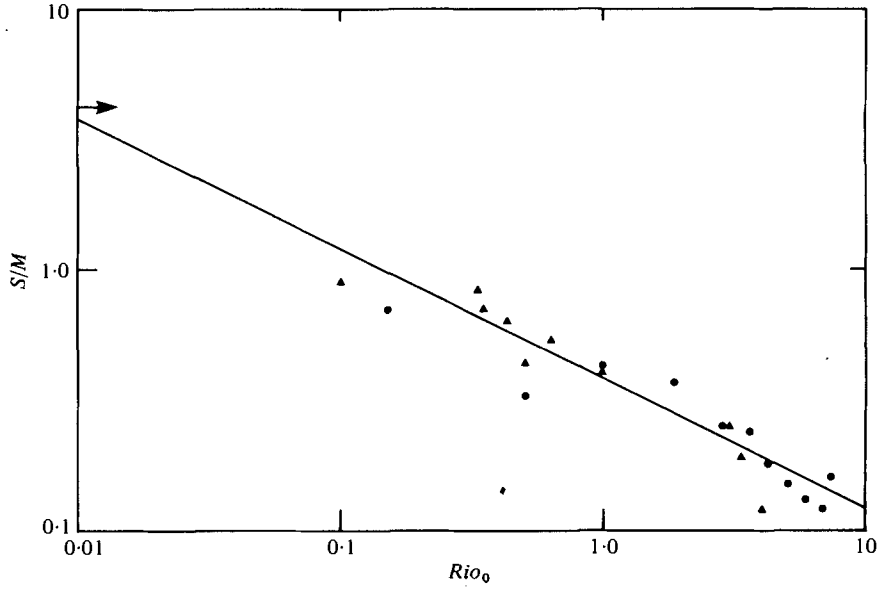

FIGURE 6. The standard deviation S of the density profiles, non-dimensionalized by the mesh length M of the grid, plotted logarithmically against the overall Richardson number Ri_0. The symbols have the same meaning as on figure 4. The straight line has a slope $-\frac{1}{2}$ and is fitted by eye to the data. The arrow on the top left of the graph represents the value of S/M determined from dispersion measurements in unstratified fluid.

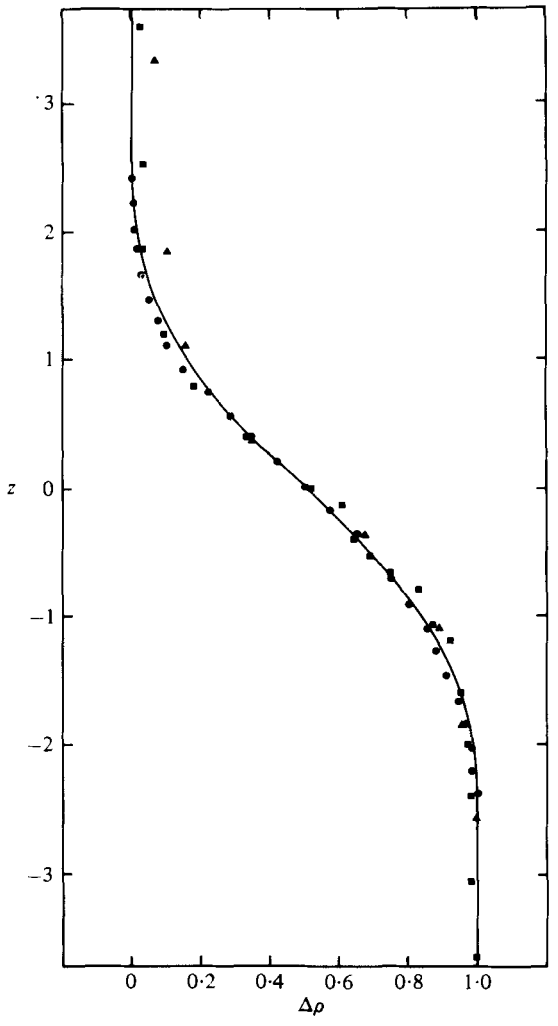

FIGURE 7. Three rescaled density profiles ●, $Ri_0 = 0{\cdot}15$; ■, $Ri_0 = 0{\cdot}98$; ▲, $Ri_0 = 5{\cdot}88$ compared with an error function. Each profile has been centred about the mean density and rescaled so that $\Delta\rho = 1{\cdot}0$ and $S/M = 1{\cdot}0$.

5. Final density profile

The passage of the grid and the subsequent mixing produced by the turbulence alters the shape and thickness of the density interface. The basic form of the stratification is unaltered in that there is still a transition region between two uniform layers (provided the tank is sufficiently deep). An example from the large tank is shown on figure 5 in which $Ri_0 = 0{\cdot}98$. This shows that the interface is thickened as a result of the mixing and that the centre of mass of the stratification is raised. Comparison of this profile with the one taken in the small tank shown on figure 2 for the smaller value of Ri_0 ($= 0{\cdot}15$) shows that final interface thickness depends on the stability of the system and the size of the grids.

In order to compare the final density profiles at different Ri_0 it was assumed that

each profile was described by an error function centred on the mean density of the two layers, and the variance S^2 of the profile was then determined. The values of S, non-dimensionalized by the mesh length of the appropriate grid, are plotted against Ri_0 on figure 6. The first point to note about this figure is that by scaling the interface thickness on the mesh size M of the grid satisfactorily collapses the data. Thus for a given Richardson number the final interface thickness is proportional to M. The data also show that the interface thickness is a function of Richardson number, with S/M decreasing with increasing Ri_0.

The appropriateness of fitting the experimental density profiles by error functions can be judged in figure 7. Three density profiles with values of the Richardson number $Ri_0 = 0{\cdot}15$, $0{\cdot}98$ and $5{\cdot}88$ are plotted against the error function. Each of the profiles have been centred about the mean density, and the variance of each has been scaled so that $S/M = 1{\cdot}0$. We see that the error function provides a good approximation to the central part of the interfaces, although at higher Richardson numbers the agreement is not so good. The departures from an error function profile at high Richardson numbers imply that there is a reduction in mixing near the centre of the interface where the density gradient is large compared with the edges where the gradient is smaller. This spatial variation in the mixing will be discussed further in § 6.

Finally, it should be noted that there is a tendency for S/M to asymptote to a constant value $\sim 0{\cdot}15$ as Ri_0 becomes large. This feature is not very clear on the log–log plot shown on figure 6 but is revealed on a linear plot of the same data. This value is roughly that of the bar size of the grid $b/M = 0{\cdot}2$, and may be an inevitable consequence of the local mixing induced by the bars as they pass through the interface.

6. Vertical diffusion coefficient

The increase in interface thickness due to the passage of the grid allows for an estimate of the equivalent vertical diffusion coefficient K_z to be made. Diffusion leads to an error function profile of the form $\mathrm{erf}\,(z/2(K_z t)^{\frac{1}{2}})$ and so K_z is related to the variance S^2 of the final density profiles by

$$K_z = S^2/2t, \tag{6.1}$$

where t is taken to be the time scale for the decay of the turbulence. Ozmidov (1965), and more recently Weinstock (1978), have argued that, in a steady-state situation,

$$K_z = c\epsilon/N^2, \tag{6.2}$$

where ϵ is the rate of energy dissipation of the turbulence, N the buoyancy frequency of the stratification and c a constant of order unity. It is difficult to make a direct comparison with (6.2) because the turbulence is decaying in these experiments, and also because N varies significantly throughout the region. However, it is possible to cast the present results in the form of (6.2) by writing $\epsilon = \beta U^3/M$ and $N^2 = g\Delta\rho/\rho M$. Then (6.1) becomes

$$K_z = \frac{M}{2\beta U t}\frac{\epsilon}{N^2}\left(\frac{S}{M}\right)^2 Ri_0. \tag{6.3}$$

This relation is of the same form as (6.2) provided

$$\frac{S}{M} = \gamma\, Ri_0^{-\frac{1}{2}}, \tag{6.4}$$

where γ is a constant, since the other term is merely a non-dimensional estimate of the decay time. The line

$$\frac{S}{M} = 0{\cdot}38\, Ri_0^{-\frac{1}{2}}, \tag{6.5}$$

is shown on the log–log plot of figure 6 and is in good agreement with the data for $Ri_0 \lesssim 2$. It seems, therefore, that for these low values of Ri_0 the rather naive assumptions such as supposing the dissipation is independent of stratification lead to a satisfactory description of the spread of the interface. Perhaps this is because $Rf \sim 0{\cdot}1$ and so the changes in ϵ are too subtle to be detected in this formulation.

It was noted earlier that there is a tendency for S/M to become roughly constant for large values of Ri_0. This deviation of S/M from (6.5), and the fact that there are significant variations from an error function density profile, implies that an eddy diffusivity K_z which is constant in space is quite inappropriate at these high values of the Richardson number ($Ri_0 \gtrsim 2$). The fact that the mixing cannot be described by a constant eddy diffusivity is the reason why the curve of Rf *vs.* Ri_0 exhibits a maximum at $Ri_0 \simeq 1$.

At the other extreme, figure 6 shows the value of $S/M = 4{\cdot}2$ estimated from dispersion in an unstratified fluid. Assuming, as seems plausible, that (6.5) holds as $Ri_0 \to 0$ we see that this value corresponds to $Ri_0 \simeq 10^{-2}$. This indicates that for $Ri_0 \lesssim 10^{-2}$ the interface is passive and the system behaves as though the fluid is unstratified. In both the small and large tanks, this implies that the density difference is passive when $\Delta\rho/\rho \lesssim 10^{-4}$.

7. Conclusions

The experiments described in this paper examine the mixing produced when a horizontal grid of bars falls through a sharp density interface. The main features can be summarized as follows.

(1) The mixing raises the centre of mass of the stratification and thickens the interface. The ultimate thickness of the interface is a decreasing function of Richardson number Ri_0.

(2) The fraction of the available kinetic energy used in mixing the fluid, the flux Richardson number Rf, is a function of Ri_0. As Ri_0 increases from zero, so does Rf which reaches a maximum value $Rf = 0{\cdot}12$ at $Ri_0 = 1{\cdot}3$. With further increase in Ri_0, Rf decreases again.

(3) The above results are independent of grid Reynolds number over the range $5100 < Re < 16000$. This range corresponds to turbulent Reynolds numbers, based on the turbulence velocities and length scales from 350 to 1200.

As was pointed out at the beginning of the paper the main aim of these experiments was to determine the form of Rf as a function of Ri_0, as this has important implications for the effects of turbulence in stably stratified fluids. The increase in Rf with Ri_0, at low values of Ri_0, results from the fact that with increasing stratification more energy is extracted from the turbulence by working against the buoyancy forces. At the maximum value of Rf, more than 80 % of the available kinetic energy is still dissipated by viscosity. For these low values of Ri_0 the mixing can be characterized by a vertical diffusion coefficient which is constant in space, and as shown by (6.2), decreases with increasing stability.

At larger values of Ri_0 the efficiency of the mixing is reduced by the buoyancy forces. This is shown in an overall sense in that Rf is reduced at higher values of Ri_0, and in detail as it is observed that the mixing can no longer be described by a diffusion coefficient which is constant in space. Instead the mixing is least in the centre of the interface where the density gradient is largest.

The experiments described in this paper are very restricted but it seems clear that this kind of experiment is a very suitable configuration for looking at a number of aspects of turbulence in stratified fluids. Only sharp interfaces have been studied and only one type of grid was used, but it is a relatively simple matter to look at interfaces with different initial thicknesses and more general forms of stratification, and to investigate more thoroughly the effects of grid geometry. Also measurements, such as those by Dickey & Mellor (1980), of the properties of the turbulence itself are very valuable.

In spite of this specialized configuration Linden (1979) has shown that the present data can be compared with that obtained in other contexts, and the simplicity of the present experiments allow parameter ranges to be covered with comparative ease.

REFERENCES

Batchelor, G. K. & Townsend, A. A. 1948 Decay of isotropic turbulence in the initial period. *Proc. Roy. Soc.* A **193**, 539.

Dickey, T. D. & Mellor, G. L. 1980 Decaying turbulence in neutral and stratified fluids. *J. Fluid Mech.* **99**, 13.

Hoerner, S. F. 1965 *Fluid-Dynamic Drag.* (Write c/o A.I.A.A. New York for author's address.)

Linden, P. F. 1979 Mixing in stratified fluids. *Geophys. & Astrophys. Fluid Dyn.* **13**, 3.

Naudascher, E. & Farell, C. 1970 Grid turbulence. *Proc. A.S.C.E., J. Engng. Mech. Div.* **96**, 121.

Ozmidov, R. V. 1965 On the turbulent exchange in a stably stratified ocean. *Bull. Acad. Sci. U.S.S.R., Atmos. & Oceanic Phys.* **1**, 257.

Pearson, H. J. 1980 Some aspects of turbulence in a stably stratified fluid: vertical diffusion and the final period of decay. Ph.D. thesis University of Cambridge.

Phillips, O. M. 1972 Turbulence in a stably stratified fluid: it is stable? *Deep-Sea Res.* **19**, 79.

Posmentier, E. S. 1977 The generation of salinity fine structure by vertical diffusion. *J. Phys. Ocean* **7**, 298.

Townsend, A. A. 1954 The diffusion behind a line source in homogeneous turbulence. *Proc. Roy. Soc.* A, **224**, 487.

Weinstock, J. 1978 Vertical turbulent diffusion in a stably stratified fluid. *J. Atmos. Sci.* **35**, 1022.

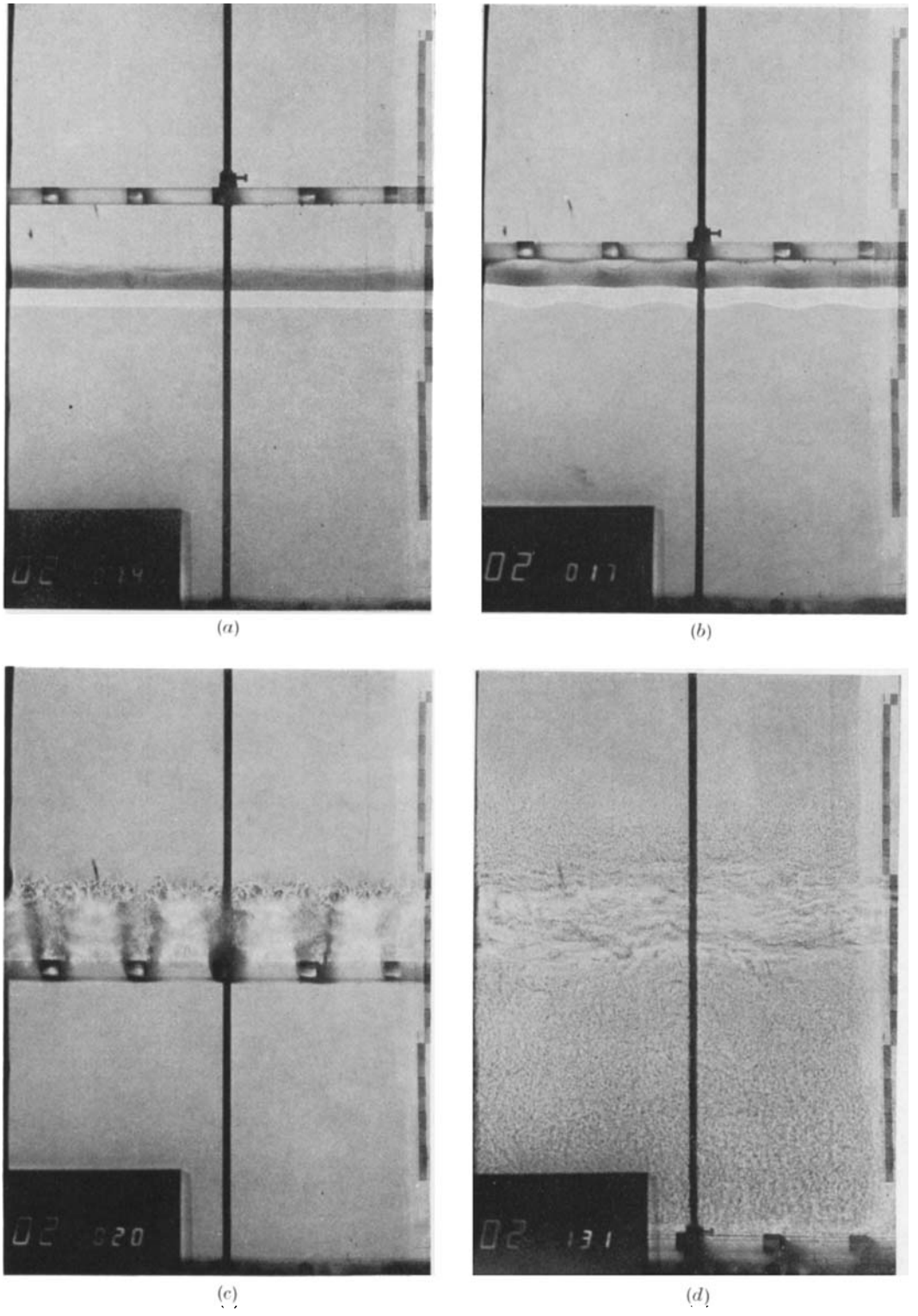

(*a*) (*b*)

(*c*) (*d*)

FIGURE 1 (*a*)–(*d*). For legend see Plate 2.

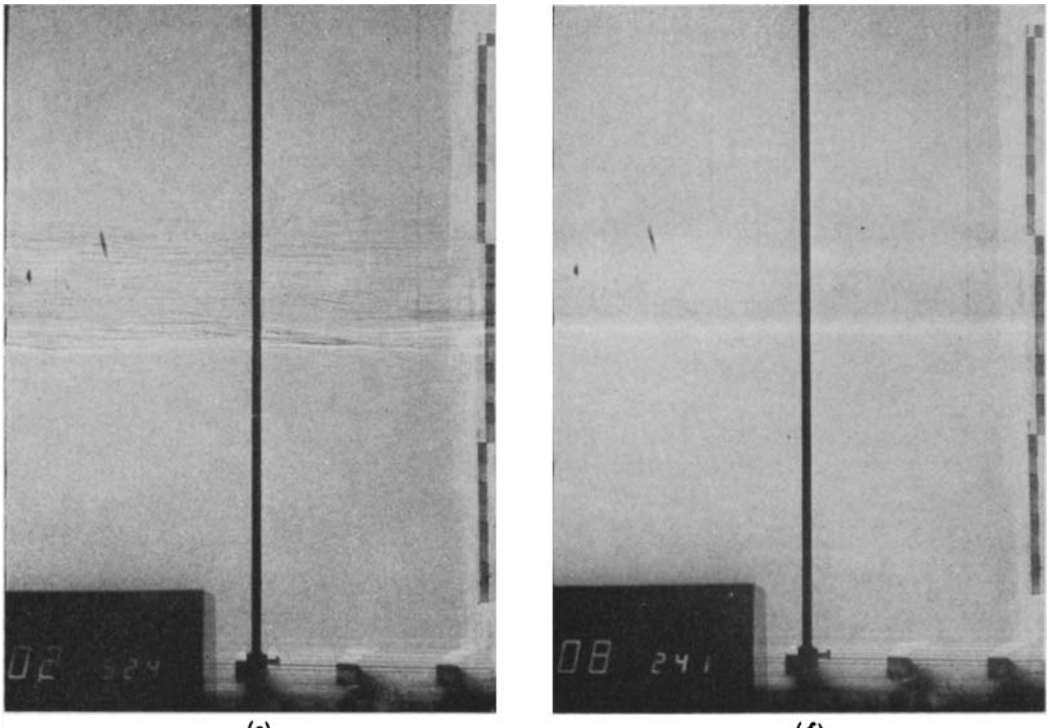

(*e*) (*f*)

FIGURE 1. A sequence of shadowgraph views of the mixing in the small tank produced by the grid as it falls through the interface for $Ri_0 = 0{\cdot}47$. The clock shows the time in minutes, seconds and tenths: the grid was released at 2 minutes on the clock. The scale on the right-hand side is in cm offset every 10 cm.

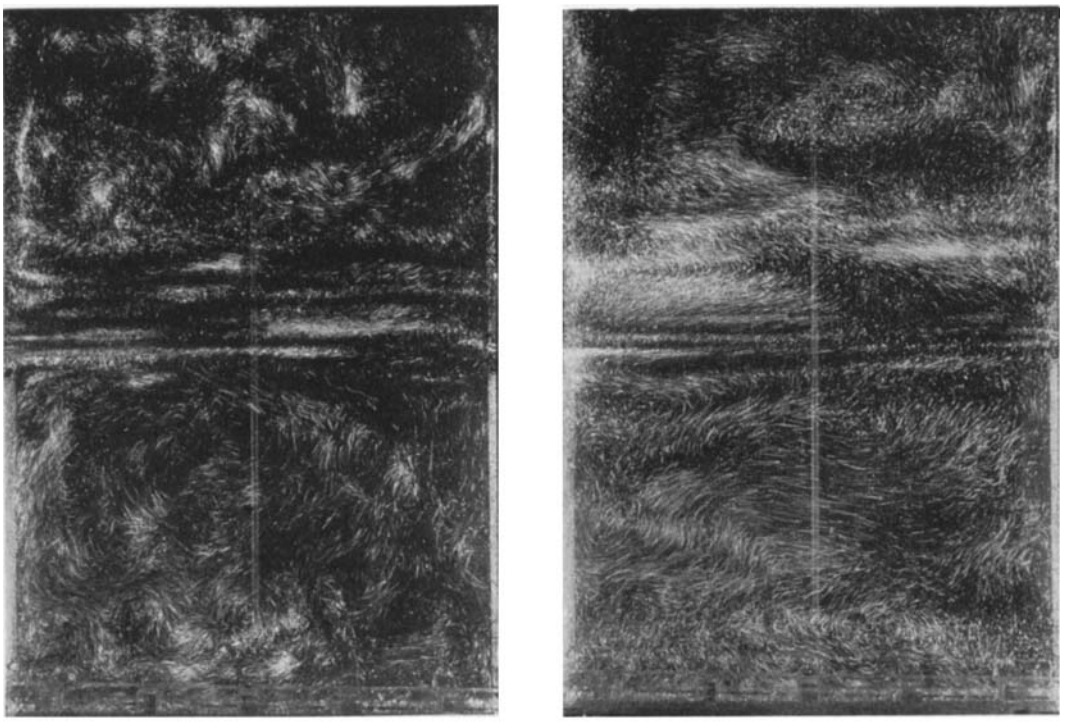

(*a*) (*b*)

FIGURE 3. Time exposures of aluminium particles suspended in the flow for $Ri_0 = 3{\cdot}63$: (*a*) 2 s exposure 20 s after grid has passed; (*b*) 8 s exposure 3 min after grid passage. The grid, visible at the bottom of the tank, provides a convenient scale as the mesh size is 5 cm. The central guide rod can also be seen on these photographs. Lighting is from the side through a vertical slit 1 cm wide.